Photonic crystal fiber polarization filter with two large apertures coated with gold layers*

Jun-Jun Wu(吴君君)[1,2], Shu-Guang Li(李曙光)[1,†], Qiang Liu(刘强)[1], and Min Shi(石敏)[1]

[1] *Physics Department, College of Science, Yanshan University, Qinhuangdao* 066004, *China*
[2] *College of Qing Gong, North China University of Science and Technology, Tangshan* 063009, *China*

(Received 13 April 2017; revised manuscript received 21 June 2017; published online 30 September 2017)

A novel photonic crystal fiber (PCF) polarization filter is designed and fabricated; it consists of two large apertures coated with gold. The asymmetric structure separates the resonance position in the vertical direction well. Due to the metal layer covering, loss is greatly improved. Finite element method is applied for numerical simulation. The influences of varying gold thickness and varying the diameters and the center positions of the larger apertures on filtering performance are evaluated. Theory of coupling between surface plasma and core mode is introduced. By modulating the parameters, we realize a single polarization filter at 1.31 μm and 1.55 μm. The basal mode loss in the *y* direction can reach 1408.80 dB/cm at 1.31 μm and 1911.22 dB/cm at 1.55 μm respectively, but basal mode loss in the *x* direction is relatively small, 0.82 dB/cm and 1.87 dB/cm. In addition, two kinds of broadband polarization filters are proposed. If the fiber length is set to 200 μm, the extinction ratio is greater than 20 dB with width of 570 nm and 490 nm. The filter has simple structure and excellent performance.

Keywords: photonic crystal fibers, polarization filter, surface plasma resonance

PACS: 42.79.Ci, 42.70.Qs **DOI:** 10.1088/1674-1056/26/11/114209

1. Introduction

Photonic crystal fiber (PCF) has been a hot topic of research over the past few years. The typical cross section has a complex refractive rate distribution, usually containing pores arranged variously. The order of magnitude of these air holes is roughly the same as the light wavelength, throughout the entire length of the device. Light waves can be limited to low refractive index fiber core propagation.[1] Compared with traditional optical fiber, PCFs have many unique physical properties that attract many scholars, such as photonic controllable nonlinear, endless single-mode, high birefringence, low loss, and big mode area.[2–6] In 2016, As_2Se_3 glass PCF with modulation instability bandwidth of up to 2738 nm was studied.[7] In 2017, a 200-μm-core-diameter Yb doped PCF with a large pitch for the air-hole cladding region was designed.[8]

With the progress of PCF manufacturing technology, various indicators of PCF performance have seen breakthrough progress, and many new products based on PCF have come into being. PCF is not only applied to the field of conventional optical communication, but is also widely applied in optical devices such as PCF sensors,[9,10] beam splitters,[11] and polarization rotators.[12] The methods of PCF fabrication are progressing. The packing method is very common. It is an improvement on the traditional optical fiber drawing process. It allows strict control of drawing tower temperature and drawing speed. At first, the basic structure of the photonic crystal fiber is designed, then the pre-melting rods are ground, and the rods are stretched to micro-tube in a drawing tower. The micro-tube is all put together in accordance with the design shape. The core is replaced by solid micro-rods which have the same diameter. The final photonic crystal fiber is formed after one or two steps of stretching.

Surface plasma resonance (SPR), which is caused by the incident electromagnetic field, has been studied extensively in recent years. Surface plasma polarization (SPP) is an electromagnetic surface wave, which exists between the dielectric and the metal interface, and can be excited by electrons or light waves. When the coupling condition is satisfied, the resonance phenomenon will take place, a part of light energy will be translated into free electrons vibration energy. With the integration of SPR technology, PCF has wider application prospects. In 2016, Li *et al.* simulated high birefringence PCF with air holes filled with fluid and coated with silver film.[13] Liu *et al.* designed a dual polarization beam splitter filled with gold, the extinction ratio is lower than −20 dB with a bandwidth of 226 nm.[14] Photonic crystal fiber polarization filters filled with metal or metal wires have been widely reported.[15–27] In 2016, Li *et al.* proposed a filter based on surface plasma resonance, with resonance intensity of 873 dB/cm at 1.05 μm; when the fiber length is 200 μm, the bandwidth of crosstalk greater than 30 dB is 170 nm. In 2016, a PCF filter filled with metal was designed. The filter model has three kinds of pores with losses of 126 dB/cm

*Project supported by the National Natural Science Foundation of China (Grants Nos. 61475134 and 61505175) and Key Program of the Natural Science Foundation of HeBei Province, China (Grant No. F2017203193).

†Corresponding author. E-mail: shuguangli@ysu.edu.cn

© 2017 Chinese Physical Society and IOP Publishing Ltd

and 326 dB/cm at 1.31 μm and 1.55 μm, with bandwidths of 20 nm and 60 nm, respectively. In 2015, Liu proposed a gold filled photonic crystal fiber polarization filter. The confinement losses are 102 dB/cm and 245 dB/cm at 1.31 μm and 1.55 μm, respectively, and the bandwidth of the loss greater than 350 dB/cm is 750 nm. In 2016, Zi *et al.* proposed a metal filled filter with square structure and two large holes. The maximum loss is 475 dB/cm, while the other direction is 60 dB/cm. when the fiber length is 1000 μm, the bandwidth of extinction ratio greater than 20 dB is 423 nm. In 2016, Liu designed a gold filled broadband filter with a square structure; the significant losses at 1.31 μm and 1.55 μm are 452.40 dB/cm and 102 dB/cm, while the undesirable losses are 0.90 dB/cm and 0.80 dB/cm. When the fiber length is 3 mm, the bandwidth of extinction ratio of more than 20 dB is 430 nm. In 2016, Dou designed a polarization filter for 1.55 μm; the useful loss can reach 630 dB/cm, and the undesirable loss is 37 dB/cm. When the fiber length is set to 2 mm, the maximum extinction ratio is 118.7 dB. In 2015, Jiang *et al.* put forward a PCF polarization filter filled with liquid crystal; the maximum loss is 433 dB/cm, and the unexpected loss is 64 dB/cm.

Here, we propose a novel PCF polarization filter. Its structure contains two large holes coated with gold film. The film is nanometer scale. Coating a large pore with a metal layer is easier than doing so for a small air hole. At the same time, its filtering characteristics are simulated by finite element method (FEM). The influence of film thickness and large air hole diameter is studied. The core of the designed PCF has high birefringence. The resonance positions of *x*-polarization and *y*-polarization modes are separated well. A single-polarization filter is realized at 1.31 μm and 1.55 μm. The loss peaks of *y*-polarization are 1408.80 dB/cm at 1.31 μm and 1911.22 dB/cm at 1.55 μm, while in *x*-polarization they are only 0.82 dB/cm and 1.87 dB/cm, respectively. The extinction character is better than that found in references.[15–27] We also produce two kinds of wide broadband polarization filters. When the length of PCF is 200 μm, with crosstalk of more than 20 dB, the bandwidths can reach 570 nm and 490 nm, better than those found in references.[15,18,19]

The experimental study was done in the following steps: (i) optimal design of PCF filter, (ii) drawing fiber samples, (iii) sample processing and analysis, (iv) making the PCF fiber, (v) data extraction and simulation of optical fiber cross-section, (vi) experimental test of filter spectra and analysis of filtering characteristics.

2. PCF structure design and the fundamental theory

Figure 1(a) shows the simple instrument in our laboratory for spectral analysis, using white light as the light source, and using common single mode fiber to connect instruments. At the same time, optical spectrum analyzer is used for spectrum measurement. Figure 1(b) is a lateral section graph of the presented filter model, which is hexagonal and composed of four layers of air holes. The center hole is removed to form a fiber core. The most obvious characteristics are two large diameter holes. The asymmetry of the structure can improve the birefringence of the fiber. The resonance position in the vertical direction can be separated. Furthermore, the two large apertures are coated with gold film inside. Due to plasma resonance, a nanoscale gold layer can greatly improve the loss in the *y* polarization direction. The air holes' pitch $\Lambda = 2$ μm. In the original structure, the diameter of the big air hole is $D = 6.6$ μm. The thickness of gold film is represented by t. The diameter of the small air apertures is $d = 1.2$ μm. The backing material is quartz. In the numerical simulation, the material dispersion of quartz and metal is considered, and the refractive index of quartz is calculated by the Sellmeier equation.[25] The dielectric constant of gold is determined by the Lorentz–Drude model[26]

$$\varepsilon_{\mathrm{m}} = \varepsilon_{\infty} - \frac{\omega_{\mathrm{D}}^2}{\omega(\omega - \mathrm{i}\gamma_{\mathrm{D}})} - \frac{\Delta\varepsilon \cdot \Omega_{\mathrm{L}}^2}{(\omega^2 - \omega_{\mathrm{L}}^2) - \mathrm{i}\Gamma_{\mathrm{L}}\omega}, \tag{1}$$

where ε_{∞} is the high frequency dielectric constant, $\Delta\varepsilon$ is the weighted coefficient, ω is the guiding optical angular frequency, ω_{D} is the plasma frequency, γ_{D} is the damping frequency, Ω_{L} represents the oscillator strength of the Lorenz oscillator, and Γ_{L} is the frequency spectrum width of the Lorenz oscillator.

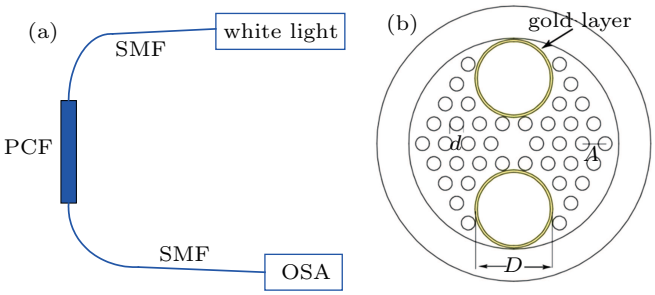


Fig. 1. (color online) (a) Experimental system device diagram and (b) cross-sectional view of the filter structure.

The mode limited loss of the fiber can be defined as[26]

$$L = 8.686 \times \frac{2\pi}{\lambda} \mathrm{Im}(n_{\mathrm{eff}}) \times 10^4. \tag{2}$$

In the above formula, the unit of limited loss is dB/cm, $\mathrm{Im}(n_{\mathrm{eff}})$ represents the imaginary part of the effective refractive index.

The fabrication of PCF has many methods, and the metal film coating technology is developing. The structure of the polarization filter we produced can be fabricated in reality.

3. Coupling theory

Because of the metal layers in large apertures, the metal plasma will couple with the light of fiber core when the matching condition of the transmission constant is satisfied. Our work starts from the study of the coupling phenomenon. We select one model as the research object. The parameters are as follows: $t = 15.6$ nm, $D = 6.6$ μm, $\Lambda = 2$ μm, $d = 1.2$ μm. It is a narrowband polarization filter. Its maximum loss can reach 1911.22 dB/cm at 1.55 μm. Figure 2 displays the transmission modes, including x polarization mode, y polarization mode, surface plasma mode, and coupled mode. The arrow represents the direction of the field. When their phases match, the basal membrane and plasma membrane will couple and a new mode will come into being. Here we explain the coupling phenomenon in theory.[27]

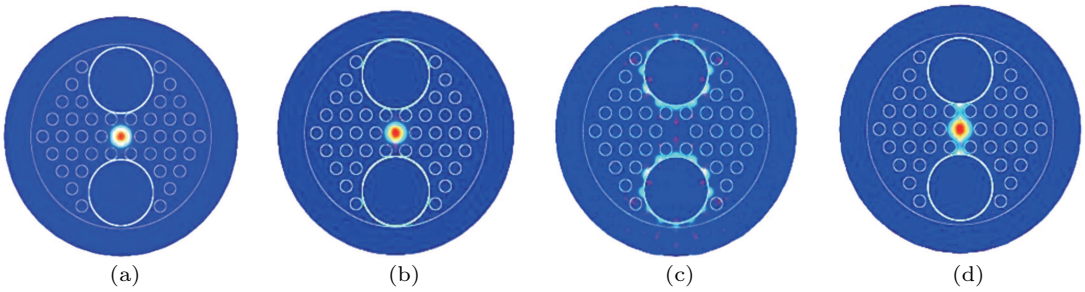


Fig. 2. (color online) Transmission modes: (a) x polarization mode, (b) y polarization mode, (c) surface plasma, and (d) the coupled mode.

When the basal mode is coupled with metal plasma, the following formulas can be used:

$$\frac{\mathrm{d}E_1}{\mathrm{d}z} = \mathrm{i}\beta_1 E_1 + \mathrm{i}kE_2, \tag{3}$$

$$\frac{\mathrm{d}E_2}{\mathrm{d}z} = \mathrm{i}\beta_2 E_2 + \mathrm{i}kE_1. \tag{4}$$

Here, β_1 is the base mode transfer constant, and β_2 represents the metal plasma transfer constant; k is the coupling coefficient, z is the coupling length. The coupling constants are expressed as β. E_1 is the electric field intensity of the base mode, and E_2 is the electric field strength of the surface plasma

$$E_1 = A\exp(\mathrm{i}\beta z), \tag{5}$$

$$E_2 = B\exp(\mathrm{i}\beta z). \tag{6}$$

We bring Eqs. (5) and (6) to Eqs. (3) and (4), then obtain

$$\beta_{\pm} = \beta_{\mathrm{ave}} \pm \sqrt{\delta^2 + k^2}, \tag{7}$$

where $\beta_{\mathrm{ave}} = (\beta_1 + \beta_2)/2$ and $\delta = (\beta_1 - \beta_2)/2$. When the transmission constant is the same, the coupling phenomenon occurs, and the core mode and the SPP transfer energy. β_1 and β_2 are not fixed values. Here δ can be written into $\delta = \delta_{\mathrm{r}} + \mathrm{i}\delta_{\mathrm{i}}$. When coupling occurs, the two modes have the same dispersion constant and $\delta_{\mathrm{r}} = 0$. So there is the formula $\delta^2 + k^2 = -\delta_{\mathrm{i}}^2 + k^2$. If $\delta_{\mathrm{i}} < k$, β_+ and β_- have different real parts, but have the same imaginary part, this is called complete coupling. If $\delta_{\mathrm{i}} > k$, β_+ and β_- have the same real part, but have different imaginary parts, this is called incomplete coupling.

Figure 3 shows the loss curveand dispersion curve with different wavelengths when coupling occurs. At phase matching position 1.55 μm, the basal membrane loss reaches maximum and the SPP membrane loss reaches minimum. Some pictures of the mode field distribution are inserted. At short wavelength, the basal membrane and SPP membrane are in the center position and metal layer, respectively. With the increase of the wavelength, the SPP mode and core mode couple to each other. But with further increase of the wavelength, the SPP mode and core mode return to their own areas again. This is a kind of incomplete coupling phenomenon.

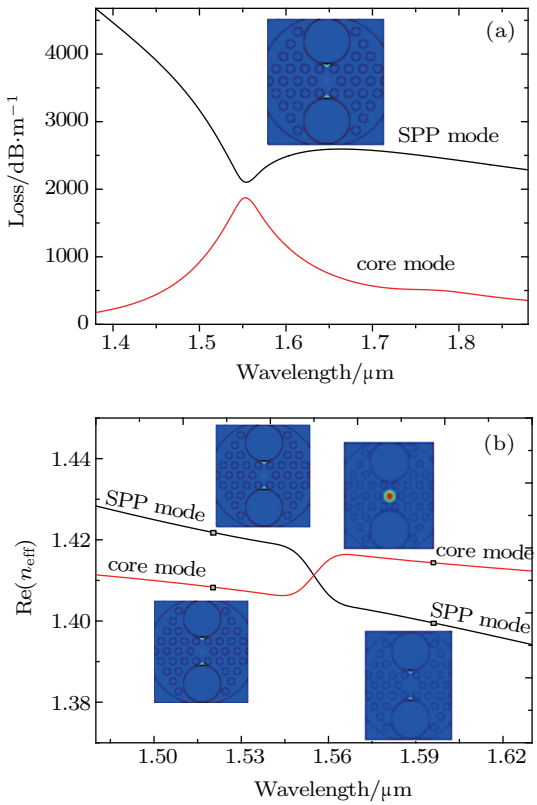


Fig. 3. (color online) (a) Loss and (b) dispersion with the change of wavelength when $t = 15.6$ nm and $D = 6.6$ μm.

4. Polarization filter

4.1. Comparing gold film thicknesses

At first, we set the big air hole diameter as $D = 6.6$ μm, the metal layers thickness $t = 16$ nm for the first attempt numerical simulation. When $D = 6.6$ μm and $t = 16$ nm, the character is good. Figure 4 illustrates the core mode loss with the change of operable wavelength λ in the y and x polarization directions. We find the loss in the y polarization direction is much larger than that in the x direction, because the air holes coated with metal film are in y direction, coupling more easily with SPP mode. The loss of resonance position 1.53 μm is 1849.87 dB/cm. But the loss of x-polarized is only 1.75 dB/cm, which is almost zero relative to the y-polarized loss. The loss of one direction is huge and another direction is small; this filtering performance is what we need.

Here we study the influence of different gold film thickness on the PCF filter features. The structural parameters are $d_1 = 1.2$ μm, $\Lambda = 2$ μm, $D = 6.6$ μm, $t = 15$ nm, 16 nm, 22 nm, 26 nm, respectively. Figure 5(a) is the relationship between loss and wavelength with different gold thicknesses. Figure 5(b) displays loss peak and resonance wavelength position with the change of gold thickness. The red, green, black, and blue solid curves depict the core mode loss in the y direction when $t = 15$ nm, 16 nm, 22 nm, 26 nm, respectively. When the gold film thickness increases, the resonant position moves to shorter waveband and the loss peak weakens. So it is not the thicker the better. We should choose reasonably according to the actual situation.

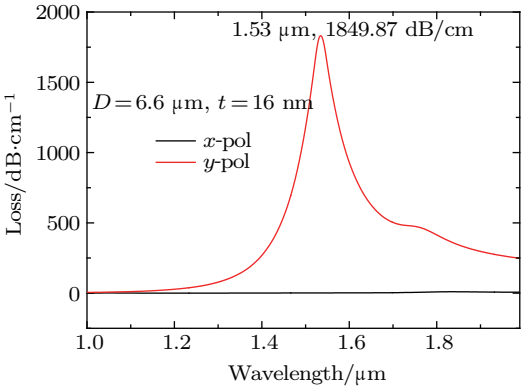


Fig. 4. (color online) Relationship between loss and working wavelength with two big air holes $D = 6.6$ μm and coated gold film $t = 16$ nm.

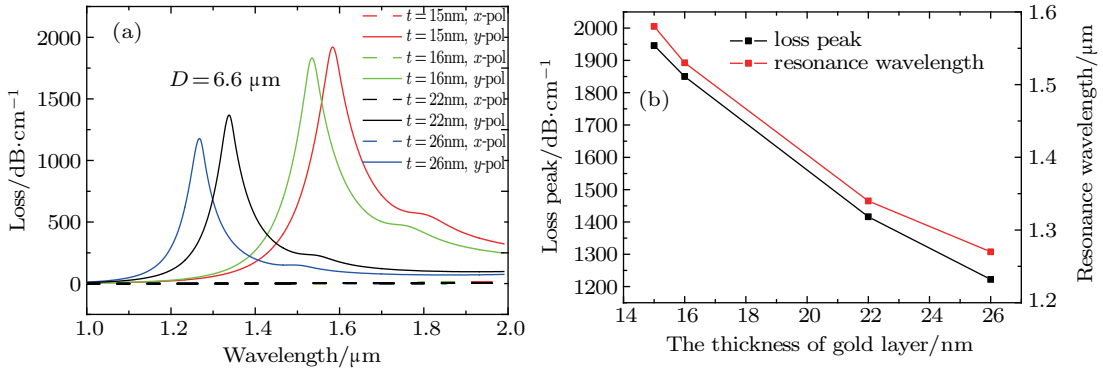


Fig. 5. (color online) (a) Loss and wavelength with different gold thicknesses. (b) Loss peak and resonance wavelength with different gold thicknesses.

4.2. Comparing diameters of the big air holes

In this part, we study the influence of different diameters of two big holes. We set two groups of parameters: $D = 6.7$ μm and $D = 6.8$ μm, the same $t = 16$ nm. In Fig. 6(a), the black and red curves depict the y direction base mode loss when $D = 6.7$ μm and $D = 6.8$ μm, respectively. When $D = 6.7$ μm, the loss peak is 1664.88 dB/cm at 1.59 μm in y polarization. When $D = 6.8$ μm, the loss peak is 1759.03 dB/cm at 1.53 μm in y polarization. But the loss in the x-direction polarization mode is only 1.63 dB/cm and 1.45 dB/cm. Moreover, the resonant position moves to a shorter waveband and the loss peak increases as the diameters of the big apertures increase.

Figure 6(b) shows the change of effective refractive index with operating wavelength when $D = 6.7$ μm, 6.8 μm. We can see that with the change of the big-hole diameter, the effective refractive index of x polarization is basically unchanged. But the effective index of y-polarization-direction mode changes significantly. Because the two big holes covered with metal film are in the y polarization direction, coupling happens between SPP and basal mode. The red curve intersects with the black curve at the resonance point where coupling happens. The effective refractive index in y-polarized mode mutates. When the big holes' diameter increases, the resonant position blue-shifts. This is consistent with the study of losses.

4.3. Single polarization filter

In this part, a single wavelength polarization filter is realized by adjusting D and t. The parameters of the designed PCF for communication band 1.31 μm are given. The air holes' pitch Λ is 2 μm, $d = 1.2$ μm, $D = 6.6$ μm, $t = 23.5$ nm. Figure 7(a) illustrates the relationship between loss and working

wavelength of the filter at 1.31 μm. We can see that the resonant wavelength is 1.31 μm. The loss peak is 1408.80 dB/cm

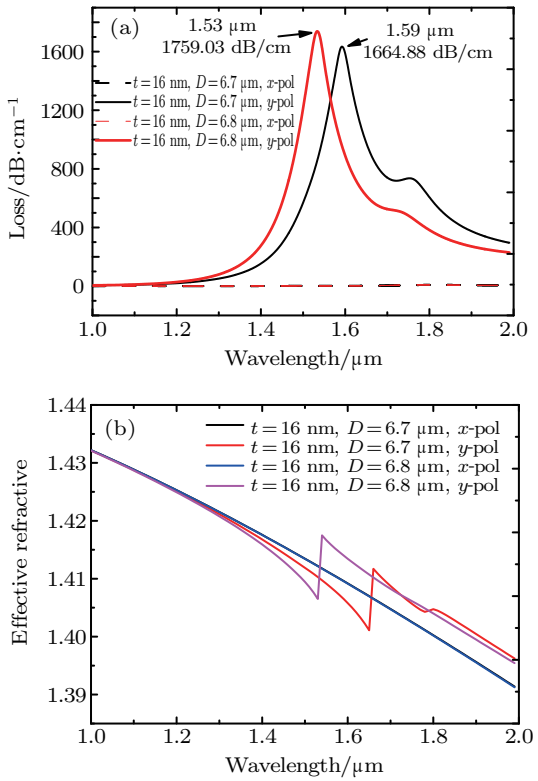


Fig. 6. (color online) (a) Relationship between loss and working wavelength when $D = 6.7$ μm, 6.8 μm and $t = 16$ nm. (b) Change of effective refractive index with operating wavelength when $D = 6.7$ μm, 6.8 μm and t=16 nm.

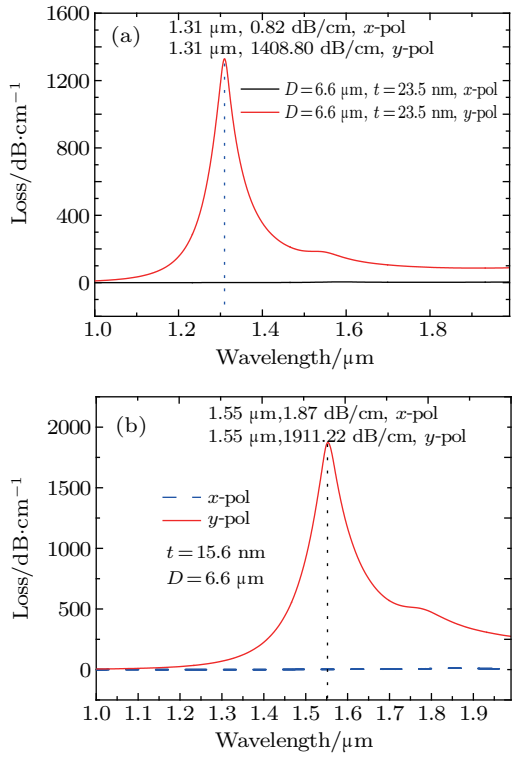


Fig. 7. (color online) (a) Relationship between loss and working wavelength when $D = 6.6$ μm, $t = 23.5$ nm. (b) Relationship between loss and working wavelength when $D = 6.6$ μm, $t = 15.6$ nm.

in y polarization direction mode, but the loss in x polarization direction is a small value of 0.82 dB/cm. This is advantageous for filtering.

The parameters of the designed PCF filter for communication band 1.55 μm are given. The air holes' pitch Λ is 2 μm, $d = 1.2$ μm, $D = 6.6$ μm, $t = 15.6$ nm. Figure 7(b) displays the relationship between loss and working wavelength of the filter at 1.55 μm. To our delight, the resonant wavelength is at communication band 1.55 μm, the loss peak is 1911.22 dB/cm in y-polarized mode while the loss of x-polarized mode is 1.87 dB/cm. There are significant differences between the two vertical losses, which is also advantageous for filtering.

4.4. Broadband polarization filter

In this part, we realize the first broadband polarization filter. The parameters of this structure are $d = 1.2$ μm, $\Lambda = 2$ μm, $D = 6.6$ μm, $t = 16$ nm. The center origin positions of the two big air holes are (0, 5.7 μm) and (0, −5.7 μm). From Fig. 8(a), we find that the loss of y polarization direction is much larger than that in the x direction, and the corresponding loss of x-polarized is very small. Because large holes coated with metal film are in the y direction, coupling with SPP mode occurs easily. Simulated data show that the loss of y-polarized is greater than 400.00 dB/cm in the wavelength range of 1.53 μm to 1.99 μm. The loss peak at 1.66 μm is 1608.60 dB/cm. The loss peak at 1.79 μm is 1391.06 dB/cm. But the corresponding loss in the x-polarized direction is only 1.79 dB/cm and 6.59 dB/cm, close to a straight line of zero in Fig. 8(a).

Crosstalk (CT) reflects the impact of a signal to another signal. It is an important measure of polarization filters and can be calculated by[28]

$$\mathrm{CT} = 20\lg\exp[(\alpha_2 - \alpha_1)L]. \tag{8}$$

Figure 8(b) shows the crosstalk measurements when the length of the fiber is 100 μm and 200 μm. The wide bandwidth of crosstalk better than 20 dB is 570 nm, from 1.42 μm to 1.99 μm. This is advantageous for making wide wavelength polarization filters.

We realize the second broadband polarization filter. The parameters of this structure are $d = 1.2$ μm, $\Lambda = 2$ μm, $D = 6.4$ μm, $t = 16$ nm. The center origin positions of the two big air holes are (0, 5.7 μm) and (0, −5.7 μm). Figure 9(a) shows the relationship between loss and working wavelength. We find the loss of the y polarization direction is much greater than that of the x direction, the undesired loss in x polarized direction is quite small. Simulated data shows that the wavelength of y polarized direction loss better than 500.00 dB/cm ranges from 1.68 μm to 1.99 μm. The losses of y-polarized are 1590.48 dB/cm and 1928.90 dB/cm at 1.76 μm and 1.95 μm. The losses of x-polarized are small values of 2.56 dB/cm

and 9.09 dB/cm. Figure 9(b) shows crosstalk when the length of the fiber is 100 μm and 200 μm. The crosstalk is better than 20 dB with a wide wavelength range from 1.50 μm to 1.99 μm. The bandwidth is 490 nm, which is also an advantage in making wide wavelength polarization filters.

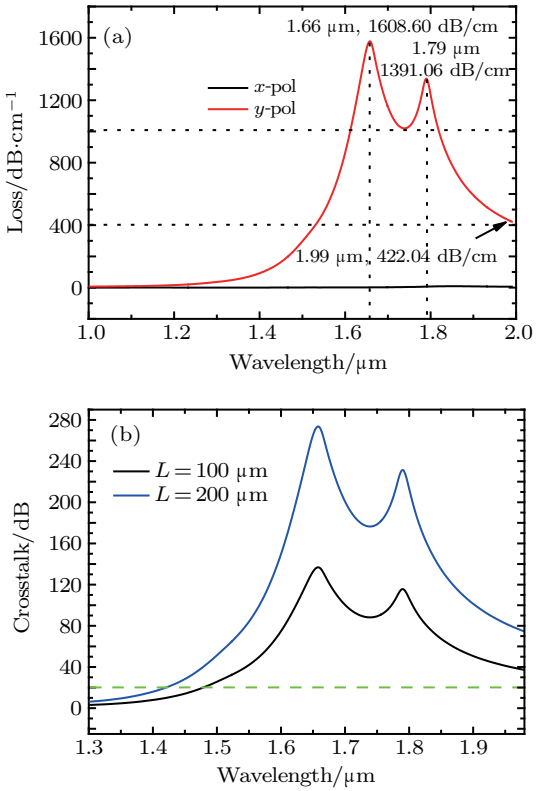


Fig. 8. (color online) (a) Relationship between loss and working wavelength when $D = 6.6$ μm, $t = 16$ nm and the center origin positions are (0, 5.7 μm) and (0, −5.7 μm). (b) Crosstalk dependence on wavelength when $D = 6.6$ μm, $t = 16$ nm and the center origin positions are (0, 5.7 μm) and (0, −5.7 μm).

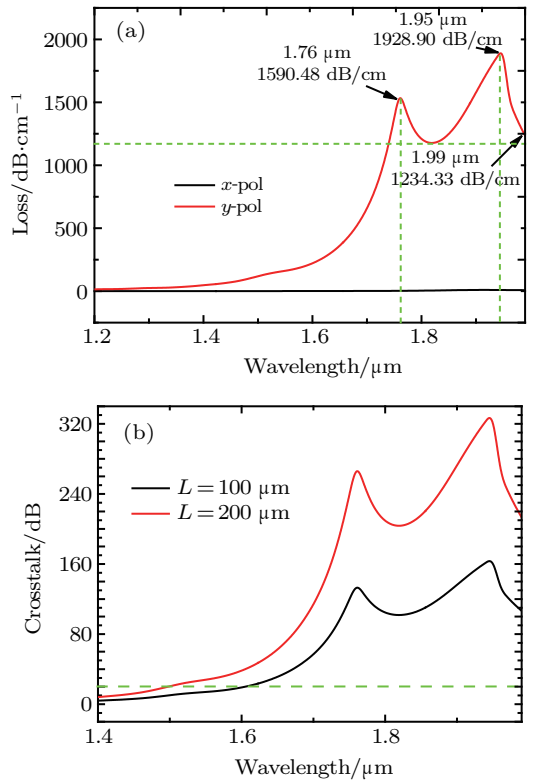


Fig. 8. (color online) (a) Loss dependence on wavelength when $D = 6.4$ μm, $t = 16$ nm and the center origin positions are (0, 5.7 μm) and (0, −5.7 μm). (b) Crosstalk dependence on wavelength when $D = 6.4$ μm, $t = 16$ nm and the center origin positions are (0, 5.7 μm) and (0, −5.7 μm).

4.5. Influence of the positions of the two big air holes

The influence of the center positions of two big air holes is discussed here. We set the centers for one sample at (0, 5.6 μm), (0, −5.6 μm); another at (0, 5.7 μm), (0, −5.7 μm). They have same $D = 6.6$ μm, $t = 16$ nm. Figure 10 shows the relationship between loss and working wavelength. The pink dotted curve depicts the base mode loss in y-polarization direction when the centers are (0, 5.6 μm) and (0, −5.6 μm). The pink solid curve depicts the core mode loss in y-polarization direction when the centers are (0, 5.7 μm) and (0 −5.7 μm). We find that when the big holes move away from the core mode, the resonance wavelength grows longer and the resonance peak decreases. This phenomenon results from gold coated holes in the y direction, where coupling occurs. With the distance between the two modes increasing, the coupling phenomenon becomes weaker. Besides, there is a broadband filtering phenomenon.

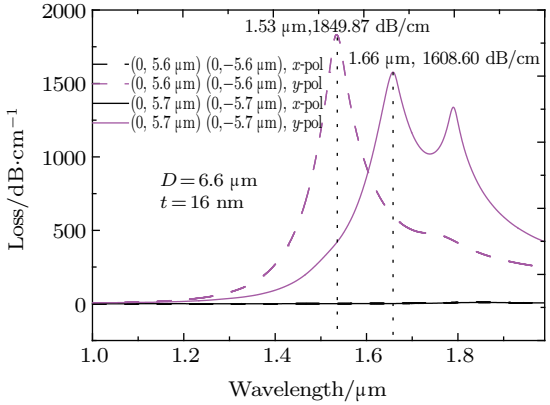


Fig. 10. (color online) Loss with the change of wavelength when $D = 6.6$ μm, $t = 16$ nm and the center origin positions are (0, 5.6 μm) and (0, −5.6 μm); and when $D = 6.6$ μm, $t = 16$ nm and the center origin positions are (0, 5.7 μm) and (0, −5.7 μm).

5. Conclusion

We design a novel polarization filter. It has two big air holes coated with gold film. If phases match, SPP mode couples to core mode. The loss in y-polarization direction is much larger than that in the x direction. Numerical simulations show that the resonant position moves to longer wave band and resonance intensity fades when the gold thickness is increased. If the big holes' diameter increases, the resonant wavelength blue-shifts and the resonance intensity strengthens. When the big holes are close to core mode, the resonant wavelength blue-shifts and the resonance intensity increases. By modulating the parameters of the polarization filter, we realize single polarization filter at 1.31 μm and at 1.55 μm. The maximal

loss in *y*-polarization is 1408.80 dB/cm and 1911.22 dB/cm, respectively, while in *x*-polarization it is only 0.82 dB/cm and 1.87 dB/cm, showing near zero in the loss diagram. Two kinds of broadband polarization filters are proposed. When the length of PCF is 200 μm, the extinction ratio is greater than 20 dB with bandwidth of 570 nm and 490 nm. The PCF has excellent performance.

References

[1] Li J S, Li S G, Zhao Y Y and Li H 2015 *IEEE Photonics Journal* **7** 1
[2] Wang X Y and Li S G 2016 *Opt. Quant. Electron.* **48** 1
[3] Liu B W, Hu M L, Song Y J, Chai L and Wang Q Y 2008 *Acta Phys. Sin.* **57** 6922 (in Chinese)
[4] Han Y, Hou L T, Zhou G Y, Yuan J H, Xia C M, Wang W, Wang C and Hou S Y 2012 *Chin. Phys. Lett.* **29** 054208
[5] Wei S U, Lou S Q, Zou H and Han B L 2014 *Acta Phys. Sin.* **50** 4216 (in Chinese)
[6] Liu S and Li S G 2013 *Chin. Phys. B* **22** 074206
[7] Wang H L, Wu B and Wang X L 2016 *Chin. Phys. B* **25** 064207
[8] Meng K, Zhu L Q and Luo F 2017 *Chin. Phys. B* **26** 054212
[9] Yang X, Lun Y, Wang W and Yao J 2016 *Opt. Commun.* **359** 279
[10] Azzam S I, Hameed M F O, Shehata R E A, Heikal A M and Obayya S S A 2016 *Optical and Quantum Electronics* **48** 1
[11] Zi J, Li S, An G and Fan Z 2016 *Opt. Commun.* **363** 80
[12] Hameed M F and Obayya S S 2014 *Opt. Lett.* **39** 1077
[13] Li R M and Zhou G Y 2016 *Chin. Phys. B* **25** 034209
[14] Liu Q, Li S, Wang X and Shi M 2016 *Chin. Phys. B* **25** 124210
[15] Zi J and Li S 2016 *Plasmonics* **11** 65
[16] Wang X Y, Li S, Liu Q, Wang G Y and Zhao Y Y 2016 *Plasmonics* **11** 6
[17] Lee H, Schmidt M, Tyagi H, Sempere L P and Russell P S J 2008 *Appl. Phys. B* **93** 111102
[18] Li H, Li S G, Chen H L and An G W 2016 *Plasmonics* **11** 1
[19] Liu Q, Li S G and Chen H L 2015 *IEEE Photonics Journal* **7** 1
[20] A Nagasaki K Saitoh and M Koshiba. 2011 *Opt. Express* **19** 3799
[21] Dou C, Jing X L and Li S G 2016 *Plasmonics* **11** 1163
[22] Jiang L, Zheng Y, Hou L, Zheng K and Peng J 2015 *Optical Fiber Technology* **23** 42
[23] Zhang X, Wang R, Cox F, Kuhlmey B T and Large M C J 2007 *Opt. Express* **15** 16270
[24] Xue J, Li S, Xiao Y, Qin W and Xin X 2013 *Opt. Express* **21** 13733
[25] Liu Q, Li S and Li H 2015 *Plasmonics* **10** 931
[26] Fan Z, Li S and Liu Q 2016 *Plasmonics* 1
[27] Wang G Y, Li S G and An G 2016 *Optl and Quantum Electronics* **48** 457
[28] Agrawal G P 1989 *Nonlinear Fiber Optics* (1st Edn.) (San Diego: Academic)